

Magnetic-field-induced microwave losses in epitaxial Bi-Sr-Ca-Cu-O films

E. Silva, M. Giura, R. Marcon, and R. Fastampa

Dipartimento di Fisica, Università di Roma "La Sapienza," piazzale Aldo Moro 2, 00185 Roma, Italy

G. Balestrino, M. Marinelli, and E. Milani

Dipartimento di Ingegneria Meccanica, Università di Roma "Tor Vergata," I-00173 Roma, Italy

(Received 11 November 1991)

Magnetic-field-induced microwave losses in epitaxial *c*-axis-oriented Bi-Sr-Ca-Cu-O films have been observed. At low magnetic field, the behavior of the absorption is qualitatively analogous to that already observed in granular samples. The dominant part is attributed to the dephasing of a network of Josephson junctions. A structural analysis shows evidence of such a network. The dependence of the absorption on the angle between the magnetic field and the *a*-*b* plane is consistent with this model.

I. INTRODUCTION

Microwave absorption has been shown to be a useful method for studying the transport properties in conventional superconducting materials. This technique has also been used to investigate the resistive properties of high- T_c superconductors with and without the presence of an external magnetic field,¹⁻¹¹ revealing the existence of weak links,²⁻⁴ glassy phenomena,^{2,5} flux flow,^{6,7} flux creep,^{8,9} phase slippage,¹⁰ and anisotropy.¹¹ The knowledge of dissipative mechanisms in high- T_c copper-oxide superconductors is of utility in the area of microwave detection, in order to make passive devices at the temperature of liquid nitrogen.

In this paper we will present a set of measurements of the microwave absorption as a function of the magnetic field in *c*-axis-oriented 2:2:1:2 Bi-Sr-Ca-Cu-O films grown by liquid-phase epitaxy and with a mosaic spread lower than 0.1°. The measurements have been taken at various temperatures and angles between the magnetic-field direction and the *a*-*b* plane. At low magnetic field ($H < 0.3$ T) the data show a behavior analogous to that found in granular samples⁴ if the magnetic field is scaled by an order of magnitude. In order to explain the experimental results, various dissipative mechanisms will be considered.

The aim of the present paper is to show that the microwave losses at low fields are dominated by the absorption due to the dephasing of the network of the Josephson junctions present in these films.

In Sec. II the experimental setup and the sample preparation are described. In Sec. III the experimental results are exposed, while a discussion of possible dissipative mechanisms is given in Sec. IV.

II. EXPERIMENTAL SETUP AND SAMPLE PREPARATION

The method of microwave surface resistance has been used to detect the losses of superconducting samples. The microwave power is fed into a rectangular cavity in which a narrow wall is substituted by the rectangular-

shaped specimen. The microwave apparatus is made sensitive to the absorption of the cavity and the power reflected from it is detected. In this condition, the reflected power is proportional to surface resistance of the superconducting film and the system allows one to measure the variation of the surface resistance. In Fig. 1 a sketch of the experimental setup is shown. The cavity is working in the TE₁₀₁ mode at the frequency $\nu = 22.5$ GHz. The microwave current density J flows in the *a*-*b* plane of the sample (vertical plane) and the magnetic field, supplied by a conventional electromagnet, rotates in a horizontal plane, so that, in our arrangement, ϑ is the angle that the H direction makes both with the J direction and with the *a*-*b* plane (inset of Fig. 1). The magnet-

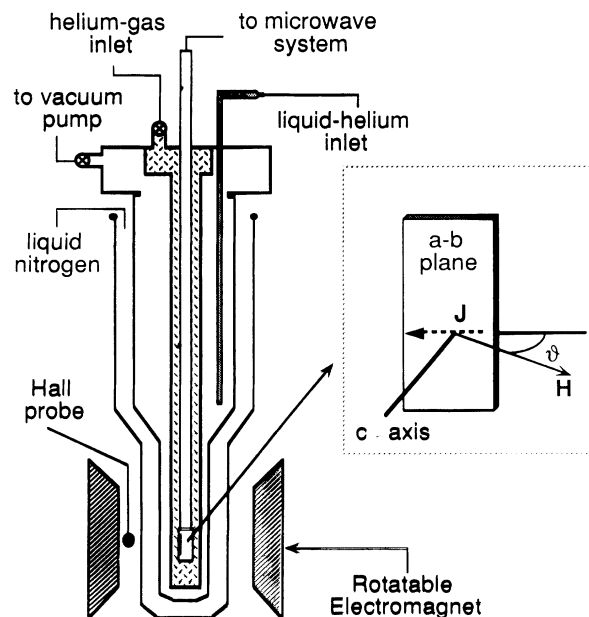


FIG. 1. Sketch of the cryogenic section of the experimental setup. In the inset, the sample arrangement with respect to the external magnetic field H and the microwave current density J is also shown.

ic field is varied in the range 0–1.3 T; the temperature is changed from 13 to 90 K and stabilized within 0.03 K by means of a resistance heater. The temperature is measured by a Pt-resistance thermometer and a Cu-Constantan thermocouple. Measurements have been performed on *c*-oriented films of 2:2:1:2 Bi-Sr-Ca-Cu-O.

Our growth apparatus is of the kind widely used for the liquid-phase epitaxy (LPE) growth of garnet films.¹² It consists of a vertical tubular furnace, with a heating zone about 0.5 m long, whose temperature is measured by a Pt/(Pt–10 at. % Rh) thermocouple, and kept stable by a Eurotherm controller. The growth solution is contained in a 100-cm³ platinum crucible, whose position can be adjusted vertically so as to obtain the desired vertical thermal gradient (see below). The substrates, kept horizontal, is attached to a Pt-Au5% holder, at the lower end of a vertical alumina rod.

The growth solution is prepared as follows. 20 g of the Bi-Sr-Ca-Cu-O constituent oxides and carbonates are mixed and put in the Pt crucible. The crucible is heated at 900°C for 1 h, and quenched in air: both calcination of the carbonates and partial melting occurs, so that a compact black mass is obtained, stuck to the crucible bottom. On top of this mass, 100 g of KCl are added, which is melted in turn, by heating the crucible again at 800°C for 1 h, followed by a further quenching. The crucible is then placed in the upper part of the heated zone of the growth furnace, so as to create in the solution a downward thermal gradient, aimed to promote the chemical transport from the solute on the crucible bottom to the top-dipped substrate.

One of the key factors influencing film growth is just the thermal gradient in proximity of the substrate, which of course is strongly dependent on the design of the substrate holder. To obtain film growth at a stable and definite temperature, the furnace thermal controller is driven by a thermocouple immersed in the liquid, in close proximity to the substrate. LaGaO₃ substrates were used.¹³

The electrical properties of films growth by the LPE technique were then investigated. The electrical resistance of the films above the transition temperature was found to have a metallic behavior with low extrapolated value at 0 K (one-tenth of the room-temperature value). The width of the dc resistive transition was 4 K and zero resistance was reached at about 80 K.

III. EXPERIMENTAL RESULTS

A. Structural characterization

The possibility of using LaGaO₃ substrates for the growth of high-*T_c* superconducting films was suggested by Sandstrom *et al.* in 1988. The main advantages of LaGaO₃ substrates over the previously used ones (MgO, ZrO₂, SrTiO₃) were shown to be the better lattice matching with the high-*T_c* superconducting compounds and the low dielectric constant. On the other hand, LaGaO₃ substrates are highly twinned, which was shown^{15,16} to result in a decrease of the current-carrying capabilities of the overlying superconducting films.

We accurately studied the twinning of (001)-oriented LaGaO₃ substrates by means of x-ray diffractometry using a conventional Bragg-Brentano diffractometer. To investigate the distribution of differently oriented grains, the detector is kept fixed to the position corresponding to the Bragg condition for the intense (0012) reflection of a 2:2:1:2 single phase Bi-Sr-Ca-Cu-O film grown on a LaGaO₃ substrate ($2\theta=40.87^\circ$ using Co *K α* radiation), while the crystal is rotated around the normal to the diffraction plane (ω scan). Different grains will therefore be in the correct position for giving a Bragg reflection for differed values of the rotation angle. From a perfect crystal, the ω scan should result in a single narrow peak. On the contrary, as shown in Fig. 2, three peaks were observed for our LaGaO₃ substrates, spaced about 0.3° and with a full width at half maximum of 0.1° each, corresponding to the instrumental broadening of our diffractometer. The presence of three separate and narrow peaks shows that the grains are not randomly misaligned with respect to one another (which would result in a single broad peak) but rather that they are aligned along three well-defined directions.

The LaGaO₃ structure is orthorhombic ($a=0.5519$ nm, $b=0.5494$ nm, $c=0.7770$ nm). However, its structure can be derived from the perovskite structure considering the original cubic cell stretched along a face diagonal so as to form a rhombus having sides of length 0.3894 nm and forming angles of 89.32° and 90.68°.¹⁷ Therefore a possible explanation of our results is that the two side peaks in the ω scan are due to grains tilted in such a way that the sides of the rhombus are perpendicular to the substrate surface [i.e., the grains are (110)- and (1 $\bar{1}$ 0)-oriented in the orthorhombic unit cell]. In these conditions the lattice spacing is 0.7787 nm, to be confronted with the *c* lattice spacing of 0.7770 nm for the (001) orientation. This difference corresponds to 0.09° only in 2θ and therefore the (001), (110), and (1 $\bar{1}$ 0) oriented grains simultaneously fulfill the Bragg condition for the

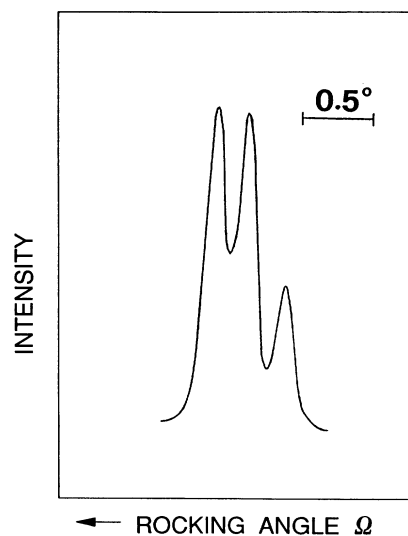


FIG. 2. Rocking curve. Co *K α* radiation for the film grown on LaGaO₃ substrate.

selected reflection. Furthermore, if this picture is correct, the angular separation of the peaks in the ω scan should vary between zero and 0.68° (the distortion of the a - b substrate grid from the rectangular shape) as the crystal is rotated around an axis perpendicular to the substrate surface, which was experimentally confirmed.

The same analysis was then performed on a bare LaGaO_3 substrate, and the same above-described features were observed in the ω scan of the (004) reflection of the substrate (Bragg angle $2\theta = 54.91^\circ$). This clearly shows, as it was expected from the fact that our films are truly epitaxial,¹⁸ that the structural properties of the film are strongly related to the substrate ones, and that the presence of twinning domains in the substrate leads to the existence of small-angle grain boundaries in the overlying film.

The surface morphology of the film was then investigated by scanning electron microscopy. As shown in Fig. 3, several cracks are observed on the film, on a 50–100- μm scale. This roughly corresponds to the spacing among twinning domains in the substrate, but the patterns of the cracks observed do not follow the twinning domains' shape, and therefore they should be attributed to thermal stresses rather than to structural causes only. Anyhow, evidence for the effects on the electrical properties of the film of the presence of grain boundaries induced by the substrate twinning comes from the large difference between the critical current densities measured on Bi-Sr-Ca-Cu-O films grown, under the same conditions, on twinned LaGaO_3 substrates and untwinned



FIG. 3. Surface morphology of the film investigated by scanning electron microscopy.

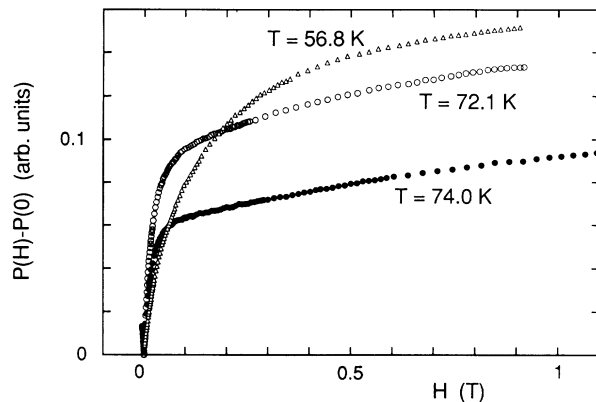


FIG. 4. Variation $P(H) - P(0)$ of the microwave absorbed power as a function of the external magnetic field H at various temperatures, with $\mathbf{H} \perp a$ - b plane. Arbitrary units remain the same in successive figures.

SrTiO_3 or NdGaO_3 substrates ($5 \times 10^5 \text{ A/cm}^2$ at 4 K for films grown on NdGaO_3 , to be compared with $3 \times 10^4 \text{ A/cm}^2$ for films grown on LaGaO_3).^{15,19}

B. Microwave absorption

The experimental results refer to the measurements of the microwave absorbed power by the superconducting films as a function of the static magnetic field at various temperature and angles between the magnetic field and the a - b plane.

1. T dependence

In Fig. 4 the variations of the microwave absorbed power as a function of the magnetic field H , at various temperatures, with \mathbf{H} directed along the c axis ($\vartheta = 90^\circ$), are shown. The measurements have the same qualitative behavior of granular Y-Ba-Cu-O and Bi-Sr-Ca-Cu-O samples, in which the existence of a network of Josephson junctions had to be assumed in order to explain the experimental results.⁴ The freezing effects depending on

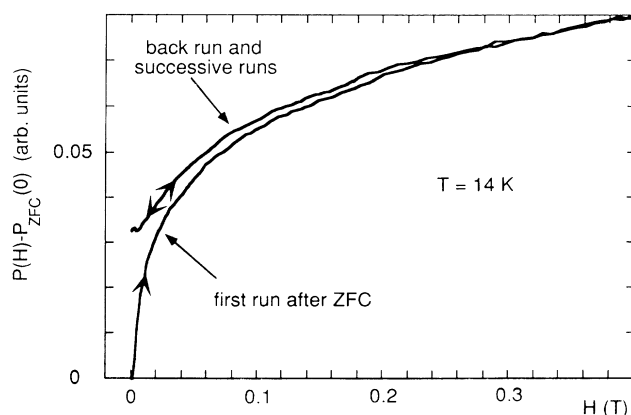


FIG. 5. Plots of the microwave absorption at low temperature for the first run in H after ZFC and for successive runs.

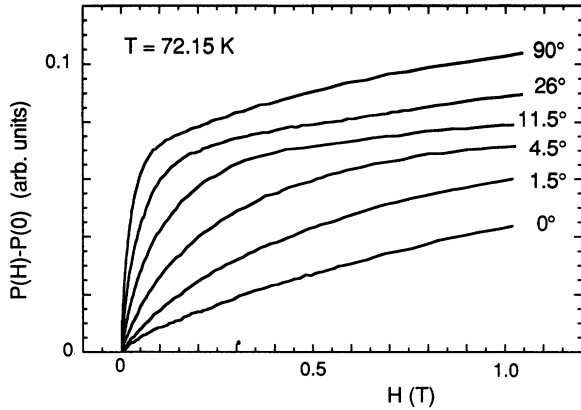


FIG. 6. Behaviors of $P(H) - P(0)$ for a fixed temperature at various angles ϑ between \mathbf{H} and the a - b plane.

the magnetic and thermal history found at low temperatures in granular samples⁵ should also be present in films. In particular, if the sample is cooled in zero magnetic field (ZFC) at a temperature sufficiently low and is successively subjected to a field H high enough (first run in H), a second run of H shows that the amplitude of the absorption is reduced. This amplitude is not modified by further applications of H (see Fig. 3 of Ref. 5). This behavior for our superconducting films at $T = 14$ K is shown in Fig. 5.

2. ϑ dependence

In Fig. 6 the variations of the microwave power as a function of the magnetic field for a fixed temperature, at various angles ϑ , are shown. As can be seen, a strong angular dependence is present in the magnetic losses. To better characterize this effect, in Fig. 7 we show that the magnetic dependence of the power absorbed scales as $\sin\vartheta$ from $\vartheta = 90^\circ$ down to a few degrees ($\vartheta = 5^\circ$) from the a - b plane. This scaling has been verified in the temperature range 60–80 K.

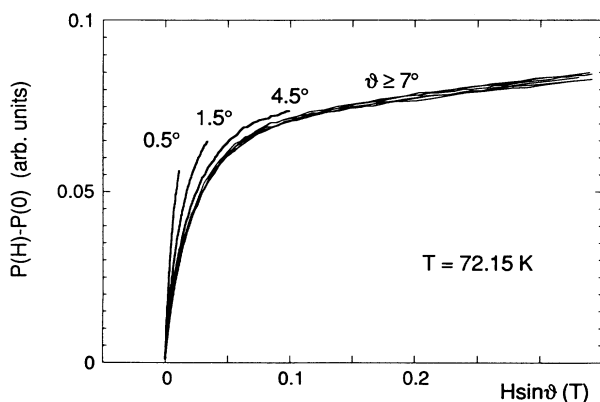


FIG. 7. Scaling of the curves of Fig. 6 as a function of $H \sin\vartheta$. In the figure only the part below $H \sin\vartheta = 0.3$ T is shown.

IV. MODELS AND DISCUSSION

In order to explain the experimental results presented in the preceding section, one must compare the different mechanisms which can give rise to dissipation in magnetic field for high- T_c superconductors. The main models for dissipation at microwave frequencies given in literature are connected to flux flow, flux creep, phase slippage, and dephasing of the Josephson junctions.

The flux-flow model refers to the dissipation due to the motion of fluxons in magnetic field, when the effect of flux pinning is negligible. In dc measurements, in order to observe the flux flow, it is necessary to impose on the sample a current density J higher than the critical current density J_c for depinning, but in ac measurements the necessity that $J > J_c$ can be avoided by choosing a frequency larger than the pinning frequency.²⁰ This frequency lies generally below the range of the microwave frequencies. The role of the flux flow in granular high- T_c superconductors at microwave frequencies has been carefully analyzed.⁷ The behavior of the power absorbed by the specimen as a function of the magnetic field is proportional to the surface resistance and is given by the expression⁷

$$P_f = a_1 \{ -1 + [1 + (a_2 H)^2]^{1/2} \}^{1/2}, \quad (1)$$

where a_1 and a_2 (which are explicitly reported in Ref. 7) are in the following assumed as parameters of the fit of experimental results. As has been shown, the flux-flow contribution in granular samples is strong enough at high temperatures ($T/T_c > 0.6$, see Fig. 3 of Ref. 7).

The flux-creep model considers the dissipation connected to the temperature-activated jumps of fluxons from the pinning centers. At the microwave frequencies, the activation energy turns out to be low,⁹ so that the absorption due to the flux creep is preeminent at low temperatures ($T/T_c < 0.5$), where irreversible effects are also present. At higher temperatures ($T/T_c > 0.6$) the creep changes into flow and the absorption becomes reversible in H .

Another dissipation model in high- T_c superconductors is due to the presence of a network of Josephson junctions (JJ), linking islands of the superconducting sample. The losses result from the voltage induced in a junction produced by the phase slippage in the presence of a magnetic field.²¹ This process is thermally activated and should be negligible at low temperatures.

The last absorption mechanics, i.e., the JJ dephasing, is also connected to the presence of links of the JJ: the application of a magnetic field changes the state of the junction to a dissipative one, so that the microwave can be absorbed. Because the JJ network is constituted by a set of junctions statistically distributed with respect to their geometrical parameters, at a fixed temperature, the variation of microwave absorbed power P as a function of the magnetic field H can be attributed to the gradual decoupling of the junctions with the increasing of H . Contrary to the slippage the amplitude of this effect should increase with the lowering of the temperature (see Fig. 4), because the lower the temperature the larger the number

of coupled junctions. This absorption, found in granular superconductors (Y-Ba-Cu-O and Bi-Sr-Ca-Cu-O) has been quantitatively discussed in a previous paper.⁴ Assuming the junctions to be mutually independent, the relative reduction of the number of coupled junctions $-(dN/N)$ is proportional to the rise dH of the magnetic field, $-(dN/N) = (H_d)^{-1}dH$, where H_d can be considered the mean decoupling field of the junctions. Then, the microwave absorbed power is given by the exponential behavior⁴

$$P_J = \Delta P_0 (1 - e^{-H/H_d}), \quad (2)$$

where ΔP_0 , the power variation when all the junctions are decoupled, is proportional to the number of coupled junctions at a given temperature.

As we will show in the following among the former proposed models of absorption only the JJ dephasing and the flux-flow mechanisms are able to explain the behaviors of the microwave power as a function of the magnetic field for temperatures higher than 50 K. At lower temperatures, the quantitative analysis of the experimental results is complicated by the freezing effects depending on the magnetic and thermal history of the sample.⁵ As a consequence, the model of mutually independent junctions ruled by Eq. (2) is no longer valid. Anyway, the freezing effects observed at low temperatures confirm the presence of a network of JJ's.

It is not possible to fit the *whole set* of experimental data of the microwave absorbed power for $T > 50$ K, as a function both of temperature and of magnetic field, without including the JJ and flux-flow contributions. Furthermore, the phase-slippage contribution is not crucial for the fit once JJ and flux-flow terms are considered. As a consequence, the analysis of the experimental data has been carried out with the functions (1) and (2). Here we do not take into account the flux-creep mechanism because of the temperature range considered (> 50 K).

In Fig. 8 we present a typical fit of the measurements,

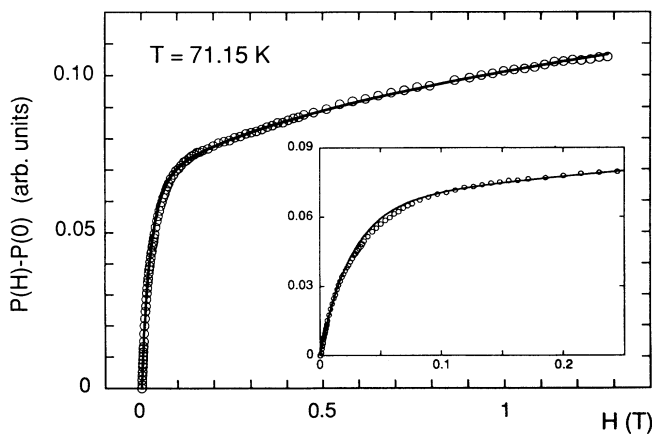


FIG. 8. Typical fit of the variation of the microwave absorbed power $P(H) - P(0)$ by means of Eq. (3) (continuous line). Open circles are experimental points. In the inset, an enlargement of the curve up to 0.2 T is shown. The magnetic field is perpendicular to the a - b plane.

obtained by means of the equation

$$P = P_f + P_J, \quad (3)$$

where P_f and P_J are given, respectively, by Eqs. (1) and (2) with ΔP_0 , H_d , a_1 , and a_2 fit parameters.

We will show in the following how the behaviors of ΔP_0 and H_d , as a function of the temperature T and of the angle ϑ , allow one to obtain information on the microscopic structure of the junction network and on the intensity of critical current. In Fig. 9, the parameters ΔP_0 and H_d are shown as a function of T (open circles). The values of H_d are an order of magnitude larger than those found in granular 2:2:1:2 Bi-Sr-Ca-Cu-O and 1:2:3 Y-Ba-Cu-O;⁴ this fact indicates that the coupling is stronger.

Under the hypothesis of the existence in the sample of a network of JJ's, it is possible to calculate the behavior of the junction parameters ΔP_0 and H_d as a function of temperature, on the line of the theory of the JJ in magnetic field. The analysis has been carried out considering the Josephson coupling energy E_J as a function of T and H :

$$E_J(T, H) = \frac{\hbar}{2e} F(T) \left\langle I_0 \left| \frac{\sin(\pi\phi/\phi_0)}{\pi\phi/\phi_0} \right| \right\rangle, \quad (4)$$

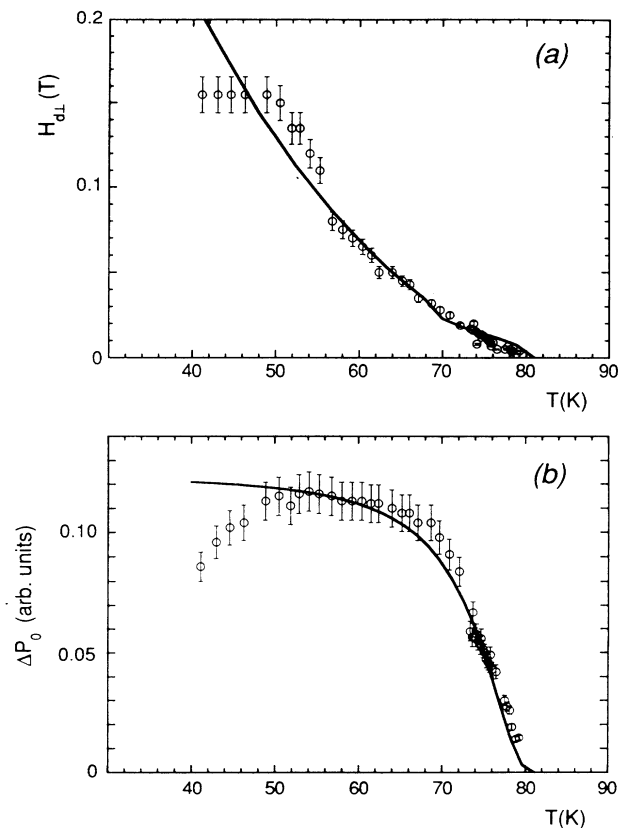


FIG. 9. (a) Behavior of the mean dephasing magnetic field H_d , (b) maximum variation of the JJ absorption ΔP_0 (open circles) when \mathbf{H} is orthogonal to the a - b plane.

where ϕ is the magnetic flux through the junction cross section, $\phi_0 = ch/2e$ is the flux quantum, I_0 is the maximum Josephson current in the junction, and $F(T)$ is a function of the temperature, which in the Ambegaokar-Baratoff theory²² is given by

$$F(T) = \frac{\Delta(T)}{\Delta(0)} \tanh \left[\frac{\Delta(T)}{2k_B T} \right],$$

with $\Delta(T)$ the temperature-dependent gap parameter and $\Delta(0)$ the gap at $T=0$. The dephasing field H_d is implicitly given by the condition

$$E_J(T, H_d) = k_B T.$$

In Eq. (4) the angle brackets mean an average on the statistical geometrical parameters of the junctions. The detailed procedure of an analogous fit is reported elsewhere.⁴

In Fig. 9(a) the fit of H_d and in Fig. 9(b) the fit of ΔP_0 as a function of temperature are superimposed (continuous lines) to the data (open circles), assuming for $\Delta(T)$ the BCS expression. As can be seen, for $T > 50$ K the theory fits the data fairly well. The fit parameters for both the curves are the magnetic-field penetration λ_0 at $T=0$, the averaged value of the junction linear dimension w , the junction averaged thickness l , and the variance σ of the statistically distributed junction linear dimensions. We have obtained $\lambda_0 = 0.16 \mu\text{m}$, $w = 0.12 \mu\text{m}$, $l = 0.01 \mu\text{m}$, and $\sigma = 0.04 \mu\text{m}$. It has to be stressed that the numerical values of λ_0 , w , and σ are critical for the fit development. The value found for λ_0 is in remarkable agreement with the value $\lambda_0 \approx 0.18 \mu\text{m}$ as reported in literature.²³ The values of w and l are much smaller than those obtained by the same procedure in granular samples: JJ's are smaller in epitaxial films, correctly reflecting the stronger coupling indicated by the higher values of H_d .

Defining T_{cj} as the temperature above which the JJ's are all dephased, from the experimental data one obtains $T_{cj} = 81$ K. It is then possible to evaluate the critical current density $J_c(0)$ at $T=0$ by means of the equation (in Système International units) (Ref. 24)

$$J_c(0) = 1.57 \times 10^{-8} \frac{T_c^2}{w^2(T_c - T_{cj})}, \quad (5)$$

where $T_c = 84$ K is the temperature of the onset of the transition.

Equation (5) gives $J_c(0) \approx 10^5$ A/cm². This value, two orders of magnitude higher than that found in granular samples $[(0.5-1) \times 10^3$ A/cm²], is of the order of the one extrapolated from dc measurements (3×10^4 A/cm²) carried out on the same specimen. Also, it is remarkable that recently critical current densities in excess of 10^4 A/cm² have been obtained in artificial JJ's of Y-Ba-Cu-O (YBa₂Cu₃O_{7-y}-PrBa₂Cu₃O_{7-y}-YBa₂Cu₃O_{7-y}).²⁵

In Fig. 10, the angular dependence of H_d is shown

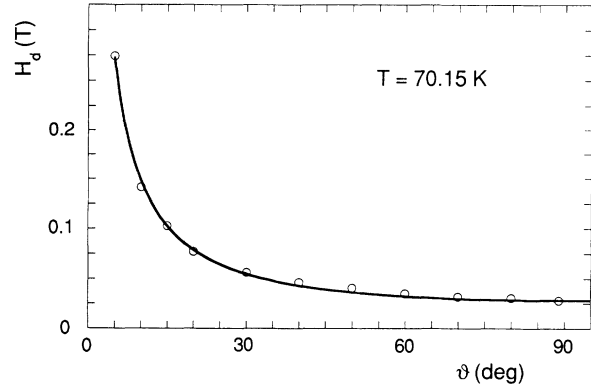


FIG. 10. Angular variation of H_d at a fixed temperature. Open circles are the points extracted by the $P(H) - P(0)$ fits, full line is obtained by the equation $H_d(\vartheta) = H_{d1}/\sin\vartheta$.

(open circles). In the same figure, the curve given by the equation $H_d = H_{d1}/\sin\vartheta$ is superimposed (H_{d1} is the H_d value for $H \perp a-b$ plane). The $\sin\vartheta$ scaling of the dephasing field H_d indicates that only the magnetic component orthogonal to the $a-b$ plane is effective. The amplitude ΔP_0 is angle independent. The angular dependence of H_d suggests that most of the junction planes are parallel to the c axis. This conclusion is corroborated by an electron microscope analysis (Sec. III A).

Preliminary measurements made on 2:2:1:2 Bi-Sr-Ca-Cu-O films, grown on untwinned NdGaO₃ substrates by the same epitaxial technique, show the same behavior of the magnetic microwave absorption but with larger H_d values, as expected from the dc higher measured values of the critical current density.

V. CONCLUSION

Epitaxial c -axis-oriented Bi-Sr-Ca-Cu-O films have been studied by means of magnetic-field-induced microwave losses. An analysis of the measurements allows us to ascribe the losses to the presence of Josephson junctions, as a consequence of the following results: (i) the exponential behavior of the microwave absorption at low magnetic field ($H < 0.3$ T), (ii) the electron microscope observation of thermal cracks parallel to the c axis of the samples, (iii) the ϑ dependence of the junction mean dephasing field H_d scaling as $\sin\vartheta$ for ϑ larger than 7° (ϑ is the angle between the $a-b$ plane and the direction of the magnetic field).

A theoretical model, based on the hypothesis of independent junctions, allows us to obtain, for temperatures larger than 50 K, the mean geometrical parameters of the junctions and to estimate the intensity of the critical current, which turns out to be of the order of that found in dc measurements.

- ¹S. Sridhar, C. A. Shiffman, and H. Hamdeh, *Phys. Rev. B* **36**, 2301 (1987); R. Durny, J. Hautala, S. Ducharme, B. Lee, O. G. Symko, P. C. Taylor, and D. J. Zheng, *ibid.* **36**, 2361 (1987); L. Cohen, I. R. Gray, A. Porch, and J. R. Waldram, *J. Phys. F* **17**, L179 (1987); A. T. Wijeratne, G. L. Dunifer, J. T. Chen, L. E. Wenger, and E. M. Logothetis, *Phys. Rev. B* **37**, 615 (1988); S. H. Glarum, J. H. Marshall, and L. F. Schneemeyer, *ibid.* **37**, 7491 (1988); J. P. Carini, A. M. Awasthi, W. Beyermann, G. Grüner, T. Hylton, K. Char, M. R. Beasley, and A. Kapitulnik, *ibid.* **37**, 9726 (1988); I. Ciccarello, M. Guccione, M. Li Vegni, and A. Sarro, *Europhys. Lett.* **7**, 185 (1988); V. F. Gantmaker, V. I. Kulakov, G. I. Leviev, R. K. Nikolaev, A. V. Polisskii, N. S. Sidorov, and M. R. Turin, *Zh. Eksp. Teor. Fiz.* **95**, 1444 (1989) [*Sov. Phys.—JETP* **68**, 833 (1989)]; S. Tyagi, A. Gould, G. Shaw, S. M. Bhagat, and M. A. Manheimer, *Phys. Lett. A* **136**, 499 (1989); S. Sridhar, D.-H. Wu, and W. Kennedy, *Phys. Rev. Lett.* **63**, 1873 (1989); B. Rakvin, T. A. Mahl, A. S. Bhalla, Z. Z. Sheng, and N. S. Dalai, *Phys. Rev. B* **41**, 769 (1990); E. J. Pakulis, R. L. Sandstrom, P. Chaudari, and R. B. Laibowitz, *Appl. Phys. Lett.* **57**, 940 (1990); K. Holczer, L. Forro, L. Mihály, and G. Grüner, *Phys. Rev. Lett.* **67**, 152 (1991); E. Silva, R. Fastampa, M. Giura, and R. Marcon, *Physica C* **173**, 145 (1991).
- ²K. Khachatryan, E. R. Weber, P. Tejedor, A. M. Stacy, and A. M. Portis, *Phys. Rev. B* **36**, 8309 (1987).
- ³M. Peric, B. Rakvin, M. Prester, N. Brnicevic, and A. Dulcic, *Phys. Rev. B* **37**, 522 (1988); G. Jung and J. Konopka, *Europhys. Lett.* **10**, 183 (1989); R. Marcon, R. Fastampa, M. Giura, and C. Maticotta, *Phys. Rev. B* **39**, 2796 (1989).
- ⁴M. Giura, R. Marcon, and R. Fastampa, *Phys. Rev. B* **40**, 4437 (1989).
- ⁵M. Giura, R. Fastampa, R. Marcon, and E. Silva, *Phys. Rev. B* **42**, 6228 (1990).
- ⁶A. M. Portis, K. W. Blazey, K. A. Muller and J. G. Bednorz, *Europhys. Lett.* **5**, 467 (1988); R. Fastampa, M. Giura, R. Marcon, and C. Maticotta, *ibid.* **9**, 719 (1989); R. Marcon, R. Fastampa, and M. Giura, *ibid.* **11**, 561 (1990).
- ⁷R. Marcon, R. Fastampa, M. Giura, and E. Silva, *Phys. Rev. B* **43**, 2940 (1991).
- ⁸E. J. Pakulis and T. Osada, *Phys. Rev. B* **37**, 5940 (1988); E. J. Pakulis, *ibid.* **39**, 9618 (1989).
- ⁹M. Giura, R. Marcon, R. Fastampa, and E. Silva, *Phys. Rev. B* **45**, 7387 (1992).
- ¹⁰H. A. Blackstead, D. B. Pulling, P. J. Mc Ginn, and J. Z. Liu, *Physica C* **174**, 394 (1991).
- ¹¹E. J. Pakulis and G. V. Chandrashekhar, *Phys. Rev. B* **38**, 11 974 (1988); **39**, 808 (1989).
- ¹²G. Balestrino, P. Paroli, B. Antonini, G. Luce, and B. Maturi, *J. Cryst. Growth* **85**, 270 (1987).
- ¹³G. Balestrino, M. Marinelli, E. Milani, A. Paoletti, and P. Paroli, *J. Appl. Phys.* **70**, 1 (1991).
- ¹⁴R. L. Sandstrom, E. A. Giess, W. J. Gallagher, A. Segmuller, E. I. Cooper, M. F. Chisholm, A. Gupta, S. Shinde, and R. B. Laibowitz, *Appl. Phys. Lett.* **53**, 1874 (1988).
- ¹⁵G. Balestrino, V. Foglietti, M. Marinelli, E. Milani, A. Paoletti, and P. Paroli, *Appl. Phys. Lett.* **57**, 2359 (1990).
- ¹⁶G. Koren, A. Gupta, E. A. Giess, A. Segmuller, and R. B. Laibowitz, *Appl. Phys. Lett.* **54**, 1054 (1988).
- ¹⁷S. Geller, *Acta Cryst. A* **10**, 243 (1957).
- ¹⁸G. Balestrino, M. Marinelli, E. Milani, A. Paoletti, and P. Paroli, *J. Appl. Phys.* **68**, 361 (1990); G. Balestrino, V. Foglietti, M. Marinelli, E. Milani, A. Paoletti, P. Paroli, and G. Luce, *Solid State Commun.* **76**, 503 (1990).
- ¹⁹G. Balestrino, V. Foglietti, M. Marinelli, E. Milani, A. Paoletti, and P. Paroli, *Solid State Commun.* **79**, 839 (1991).
- ²⁰J. I. Gittleman and B. Rosenblum, *Phys. Rev. Lett.* **16**, 734 (1966).
- ²¹M. Tinkham, *Phys. Rev. Lett.* **61**, 1658 (1988).
- ²²V. Ambegaokar and A. Baratoff, *Phys. Rev. Lett.* **10**, 436 (1963); **11**, 104 (1963).
- ²³A. P. Malozemoff, L. Krusin-Elbaum, and J. R. Clem, *Physica C* **162-164**, 353 (1989).
- ²⁴J. R. Clem, *Physica C* **153-155**, 15 (1988).
- ²⁵J. B. Barner, C. T. Rogers, A. Inam, R. Ramesh, and S. Bersey, *Appl. Phys. Lett.* **59**, 742 (1991).

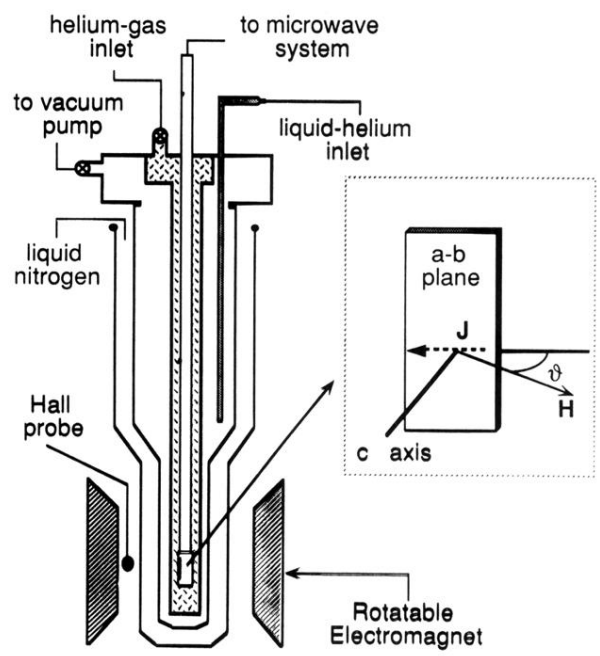


FIG. 1. Sketch of the cryogenic section of the experimental setup. In the inset, the sample arrangement with respect to the external magnetic field H and the microwave current density J is also shown.



FIG. 3. Surface morphology of the film investigated by scanning electron microscopy.